

Mechanical and microstructural behaviour of 2024–7075 aluminium alloy sheets joined by friction stir welding

P. Cavaliere^a, R. Nobile^a, F.W. Panella^{a,*}, A. Squillace^b

^a*Dipartimento di Ingegneria dell'Innovazione, Università di Lecce, Via per Arnesano, I-73100 Lecce, Italy*

^b*Dipartimento di Ingegneria dei Materiali e della Produzione, Università di Napoli Federico II, Italy*

Received 4 April 2005; accepted 7 July 2005

Available online 21 September 2005

Abstract

The aim of the present work is to investigate on the mechanical and microstructural properties of dissimilar 2024 and 7075 aluminium sheets joined by friction stir welding (FSW). The two sheets, aligned with perpendicular rolling directions, have been successfully welded; successively, the welded sheets have been tested under tension at room temperature in order to analyse the mechanical response with respect to the parent materials. The fatigue endurance (S–N) curves of the welded joints have been achieved, since the fatigue behaviour of light welded sheets is the best performance indicator for a large part of industrial applications; a resonant electro-mechanical testing machine load and a constant load ratio $R = \sigma_{\min}/\sigma_{\max} = 0.1$ have been used at a load frequency of about 75 Hz. The resulted microstructure due to the FSW process has been studied by employing optical and scanning electron microscopy either on ‘as welded’ specimens and on tested specimen after rupture occurred.

© 2005 Elsevier Ltd. All rights reserved.

Keywords: Friction stir welding; Dissimilar materials; Microstructure analysis; Fatigue tests; Mechanical properties.

1. Introduction

The Friction stir welding (FSW) technology is being widely considered by the modern aerospace and automotive industry for high-performance structural demanding applications [1]. Such joining process is demonstrated to avoid severe distortions and the generated residual stresses are proved particularly low, compared to the traditional welding processes [2–4]. The FS Welded material produces three different areas: the weld nugget, the thermo-mechanically affected zone and the external heat affected zone. The microstructural grain structure in the weld nugget is usually very fine and equiaxed, ensuring elevated mechanical strength and ductility [5,6]. In fact, some authors showed the microstructure in the weld nugget zone to undergo a continuous dynamic recrystallization process [7], leading to elevated mechanical properties.

In the FSW process, a special tool mounted on a rotating probe travels down through the length of the base metal plates in face-to-face contact; the interference between the welding tool and the metal to be welded generates the plastically deformed zone through the associated stirring action. At the same time, the thermo-mechanical plasticized zone is produced by friction between the tool shoulder and the top plate surface and by contact of the neighbour material with the tool edges, inducing plastic deformation [8]. The probe is slightly shorter than the thickness of the workpiece and its diameter is typically equal to the workpiece thickness [9]. This advanced technology is capable to weld aluminium alloys difficult to be welded with traditional fusion techniques (the 2XXX series alloys show limited weldability, whilst 7XXX series largely employed in aerospace applications are also claimed to be not easily welded). Dendrite structure occurs in the fusion zone due to conventional TIG and laser welding, leading to a drastic decrease of the mechanical behaviour [10]. The FSW process is a solid-state process, therefore the solidification micro-structure is absent in the welded metal and the presence of brittle inter-dendritic and eutectic phases is avoided [11].

* Corresponding author. Tel.: +39 0832 297278; fax: +39 0832 297279.
E-mail address: francesco.panella@unile.it (F.W. Panella).

In addition, such technology allows joining with good results aluminium based metal matrix composites, since the problems related to reinforcing particles debonding are avoided and the welded material leads to a recrystallized microstructure with elevated mechanical properties with respect to the parent material [12].

Some aluminium alloys can be welded with electrical resistance techniques, provided that an extensive surface preparation and the oxide formation is controlled. On the contrary, FSW can be used with success to weld most of Al alloys considering that superficial oxide generation is not deterrent for the process and no particular cleaning operations are needed before welding.

Other crucial aspects are the brittle solidification phases presence and the porosity formation subsequent to fusion welding; these problems are generally overcome by the FSW technique. More in detail, during FS Welding the workpiece does not reach the melting point and the mechanical properties in terms of ductility and strength of the welded zone are expected to improve if compared to the classical welding techniques [13–15]. It is remarkable how the FS Welded components are characterized by low distortion and misalignment effects, lower residual stresses amount and lack of defects induced by porosity; intergranular cracks and precipitate coalescences, with the consequence of retained dimensional and mechanical stability, are easily avoided.

The friction stir welding technology is expected to be introduced also to replace the fastener, riveted and arc welding joining methods for large scale production applications. At present time, Friction Stir Welding is mainly used to join similar materials; on the other hand, few systematic studies have been done to observe the effect due to material dissimilarity [16–19]. Actually, the demand of Aircraft Industries to substitute the conventional joining technologies with low costs and high efficient processes such as friction stir welding is considered as one of the most encouraging design challenge for the future.

FSW is increasingly becoming a useful and promising approach to face automotive and aerospace structural joining difficulties. Both in commercial and military applications, the necessity to produce welded aluminium structural sheets with elevated and reliable tensile and fatigue properties are extremely crucial. In particular, the actual need to implement advanced joining technologies for the 2XXX and 7XXX aluminium sheet alloys is directly related to the material choice for the future modern aircraft.

The aim of the present study is to investigate on the achievable mechanical and micro structural properties of dissimilar FS butt Welded sheets made up with 2024-T3 and 7075-T6 aluminium alloy with the joining line perpendicular to the rolling direction.

2. Experimental procedure

Dissimilar 2024 and 7075 Al welded alloy sheets, respectively in the T3 and T6 conditions, have been produced by Friction Stir Welding. Both the sheets measured 2.5 mm thickness. The longitudinal direction of the FSW line was perpendicular to the rolling direction of the 2024 alloy and parallel to the rolling direction of the 7075 alloy; this joint choice has been selected to simulate the most severe mechanical combination with respect to the conventional reference welding trials found in literature, in which both the sheets are welded with the same extrusion direction. The welding speed was set to 2.67 mm/s, according to optimised weldings parameters determined so far; the welding tool was fixed to the rotating axle in the clockwise direction while the parts, fixed at the backside, have been translated. The tool nib was 6 mm diameter and 2.5 mm long; a 20 mm diameter shoulder has been machined perpendicular to the tool axis; the tilt angle of the tool was set to 3°.

The Vickers hardness profile of the welded zone has been measured on the weld cross-section using a Vickers indenter with 200 gf load for 15 s. Mechanical tests have been executed on specimens having calibrated dimensions of 40 mm in length and 16 mm in width. All the specimens were obtained by means of Electrical Discharge Machine (EDM). The axial applied load was perpendicular to the weld line. Tensile tests have been performed in order to evaluate the static properties of the welded joints. They have been executed at room temperature using an MTS 810 servo-hydraulic testing machine having a load capacity of 100 kN; the cross-head speed is set to 0.1 mm/min, according to the ASTM-E8 standard code, an accurate extensometer of type MTS 634.12F-24, 25 mm base length, has been used.

High cycle fatigue tests have been performed on a resonant electro-mechanical testing machine in order to accelerate the testing time up to 250 Hz wave loading control. The TEST-TRONIC 50 ± 25 kN, produced by RUMUL has been used.

The fatigue tests have been executed in axial stress-amplitude control mode ($R = \sigma_{\min}/\sigma_{\max} = 0.1$). Due to the specimen compliance mounted in the flexible grips, the working frequency was 75 Hz. All the tests have been conducted to failure and the specimen design respects the standard requirements (the welded profile has not been polished). Successively, the significant rupture surfaces have been prepared by standard metallographic techniques and etched with Keller's reagent, in order to study the grain structure of the welded zones and to allow optical microscopy characterization. In addition, a scanning electron microscope equipped with field emission gun (type JEOL-JSM 6500 F) has been employed to observe the specimens surfaces of fracture either with monotonic and cyclic load; the microscopic morphology and defects of

the welded joints and the mechanics involved during tensile and fatigue failure have been analysed.

3. Results and discussion

3.1. Metallurgical analysis

In the present study, the dissimilar materials 2024 and 7075 aluminium alloys have been successfully joined with the FSW Process and no visible superficial porosity or macroscopic defects have been observed on both the top and rear welded surfaces.

Light microscopy observations have been done on the welded specimen cross-sections (Fig. 1); the FSW Process applied on dissimilar 2024 and 7075 aluminium alloys revealed the classical formation of the elliptical ‘onion’ structure in the centre weld; this is confirmed by the microstructure with fine recrystallized grains. The Thermo-Mechanical Affected Zone (TMAZ) is also distinguished through optical microscopy.

The micro hardness profile along the FS Weld is shown in Fig. 2, in which a value of 150 Hv is reached in the centre weld; the micro hardness profile increases in both the 2024 and 7075 sides and then starts to descend after 2 mm from the centre until reaching the hardness corresponding to the parent materials. It can be noticed the welded joint hardness to assume lower values in the HA Zone with respect to both the 2024 and 7075 parent material sides; this is in respect of the classical behaviour for aluminium alloys welded by FSW.

Fig. 3 represents the ‘nugget’ zone at a distance of 2 mm from the weld centre at the AA2024 side, which consists of fine and equiaxed grains. The higher temperatures and severe plastic deformations result in remarkable smaller grains compared to the base metal, according to all the FSW literature data for aluminium alloys; the initial elongated

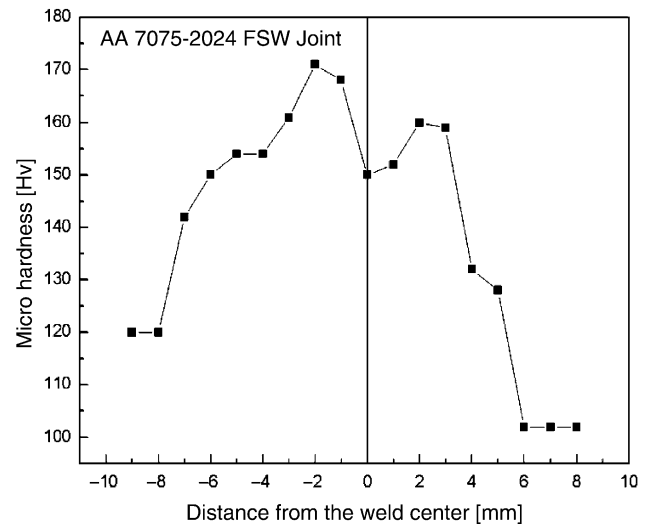


Fig. 2. Microhardness profile measured in the joints of the 2024–7075 FSW plates, AA7075 side on the left.

grains of the parent materials are mechanically converted to a new equiaxed fine grain structure. At higher magnifications, the optical micrographs show extremely fine and equiaxed grains in the recrystallized zones (estimated length $< 3 \mu\text{m}$).

Focussing away from the weld centre part at the AA7075 side, the grain dimension considerably increases and the orientation results with a less equiaxed character (Fig. 4). In particular, at a distance of 4 mm from the weld centre, a large amount of resident parent material grains start to appear. This region corresponds to the Heat Affected Zone, where the hardness is low with respect to the base metal. In fact, the precipitates in this area are coarsened as discussed by Jata et al. [4]. In the region adjacent to the nugget, i.e. TMAZ, no recrystallization apparently occurs because of the low temperature field originated by the Friction Stir process. Fig. 5(a) shows the deformed grains in the TMAZ

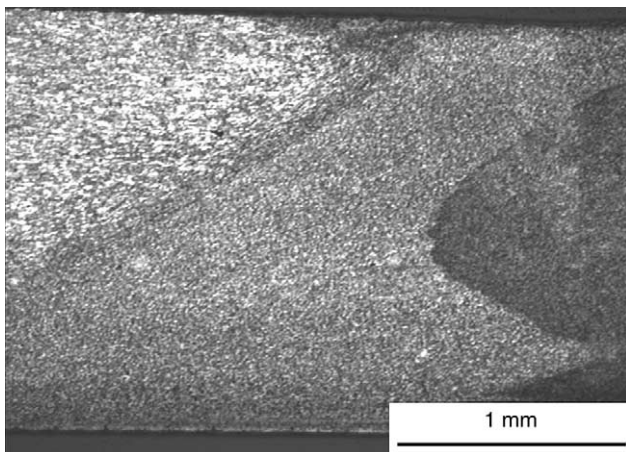


Fig. 1. Cross section of the welded specimen: particular of the nugget zone, TMAZ and base material interface.

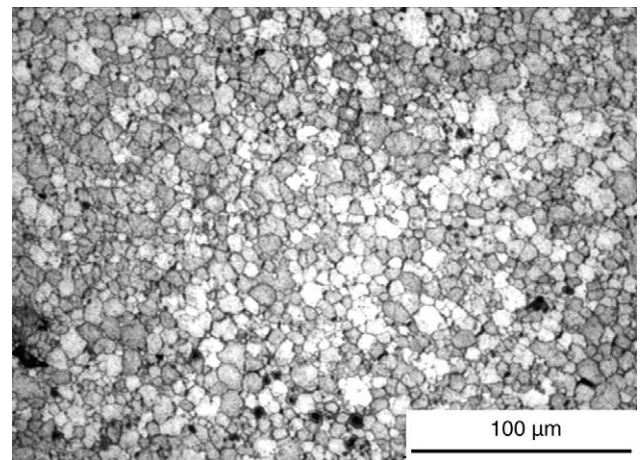


Fig. 3. Fine recrystallized grains observed at a distance of 2 mm from the weld centre of the studied joints at the AA2024 side.

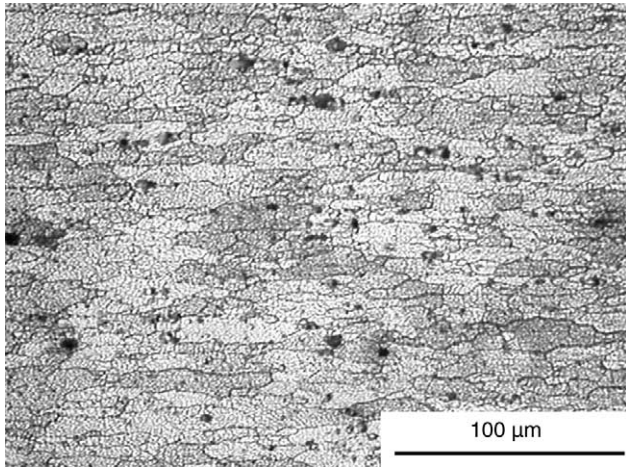


Fig. 4. Grains of parent material appearing at a distance of 4 mm from the weld centre of the joints at the AA7075 side.

and the regions adjacent to it, while Fig. 5(b) confirms the grain size to be similar to the base metal. However, the hardness in the HAZ is limited in low ranges. Similar microstructural behaviour has been observed in the FSW zone of the 2024 alloy side of the weld.

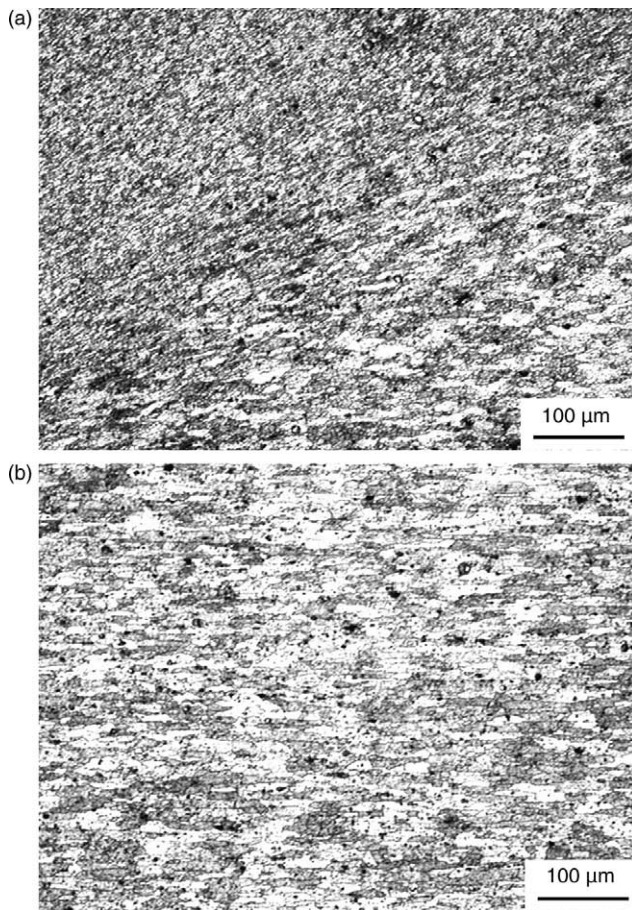


Fig. 5. TMZ zone grains (a) and parent material grains (b) at the AA7075 side: the grains dimensions difference is clearly distinguished in the studied joints.

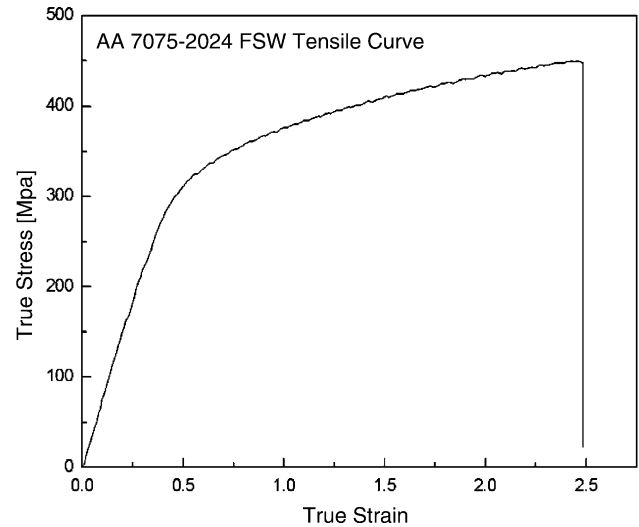


Fig. 6. True stress vs. true strain curve of the FSW joint in tension.

3.2. Mechanical characterization

The static response of all the 2024 and 7075 dissimilar sheets joined by FSW is described in Fig. 6. The traction curves show a classical and remarkable behaviour; the mechanical properties, compared to the parent metals, are reported in Table 1. The joints exhibit very good ductile properties after yielding and the Ultimate Tensile Stress is settled at high levels. Even that the FS Welded specimens show lower proof stress at 0.2% and limited total elongations with respect to the base metals, the mechanical results are extremely good considering the drastic conditions to which the materials are subjected during the Friction Stirring process.

All the tested specimens fractured beside the weld HAZ zones, close to the 2024 material side. This is in accordance with the behaviour of dissimilar welded sheets in which, from a microstructural point of view, the mechanical response of the centre weld results higher than the parent material and the HAZ because of the grain dimension differences and the precipitates concentration at the interfaces. In the lateral zones, in fact, the mean grain equivalent diameter resulted from the optical images to be around 2.5 μm.

The Wöhler curves originated by the fatigue tests data are reported in Fig. 7; the fatigue results show the characteristic behaviour for dissimilar aluminium sheets, showing a trend of fatigue life decreasing with the stress

Table 1
Mechanical properties of the 2024–7075 joints compared with those of the parent materials

Material	σ_y (MPa)	UTS (MPa)	Elongation (%)	E (GPa)
AA2024	380	490	17	72.4
AA7075	503	572	11	71
2024–7075 FSW	325	424	6	54

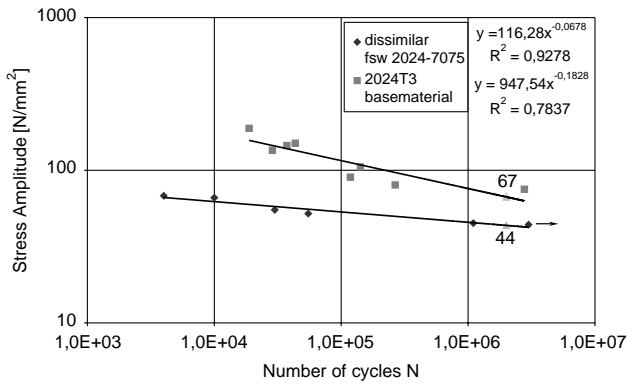


Fig. 7. Endurance Fatigue curve (S–N) of the 2024–7075 plates joined by Friction Stir Welding.

amplitude with an average slope particularly elevated even for a typical ductile alloy. Since aluminium alloys display fatigue limits at very high number of cycles (normally $> 10^7$) and even more but the main goal is to estimate the fatigue behaviour at high stress regime, the tests have been conducted to produce rupture at relatively short times (around 10^6 cycles) rather than at greater number of cycles. According to these considerations, the fatigue strength of the welded joints can be expressed as the stress amplitude level at a given number of cycles, a fatigue life of 2×10^6 cycles, which is found to be around 44 MPa, as recorded for the dissimilar FS Welded joints of the present work.

The fatigue curves show good and consistent results, since a low scatter band is observed given that few specimens have been tested (Fig. 7). Over more, the data compared with the typical alternate stress levels for the parent material at the same test frequency seem to be positioned at a lower but acceptable and interesting level, considering the severe and critical conditions exhibited by aluminium welded joints subjected to cyclic loading. Finally, the fatigue properties can be incremented by heat

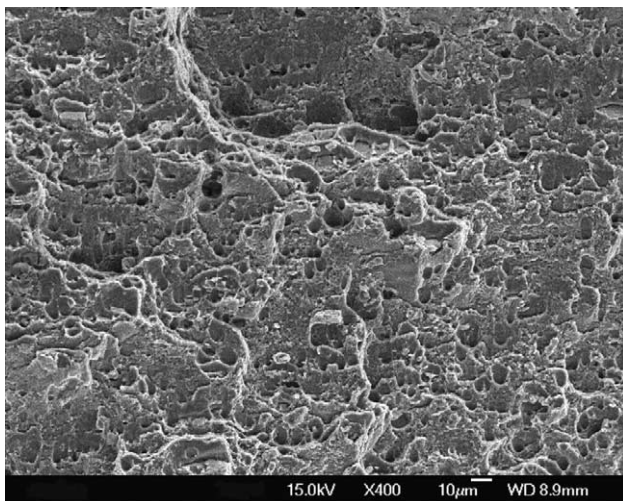


Fig. 8. Tensile specimen fracture surface of the studied joint showing voids population.

treatments, re-precipitation, and hardening processes in the TMAZ.

3.3. Fracture surfaces analysis

A better comprehension and understanding of the mechanical fracture and defect nucleation properties are strongly dependent on purposed analyses of the rupture surfaces, since the influence of the microstructural morphology of the welded interfaces on the endurance time results to be fundamental. Several interesting observations have been done.

The fracture surface of the welded 2024–7075 specimens tested under tension resulted to be covered with a broad population of microscopic voids of different size and shape (Fig. 8); at room temperature the material showed ductility to occur within the fracture progression and the observations performed by employing FEGSEM confirmed the presence of locally ductile mechanisms.

In particular, two different types of dimples have been observed, those immediately close to the voids (Fig. 9a)

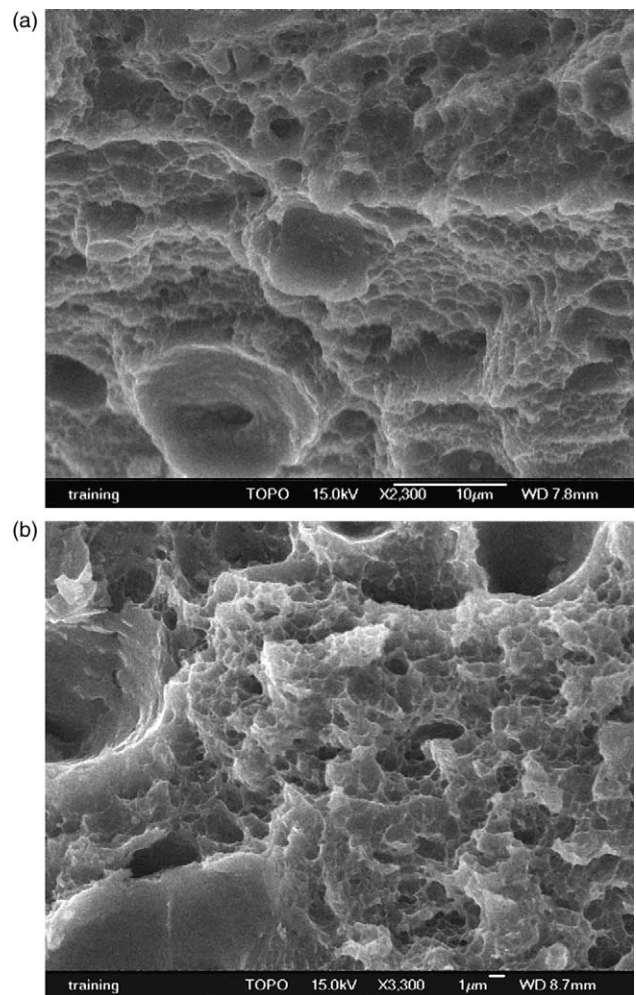


Fig. 9. Dimples showing ductility behaviour of the AA 2024–7075 FSW joints close to the voids (a) and the precipitates (b).

and those associated with the second phase coarse particles and precipitates, which resulted much smaller and shallower (Fig. 9b).

With the rapid increasing of FSW technology in various applications, the investigation of fatigue and fracture behaviour in the low and high cycle regime represents an important task to validate the process; in addition, the fractography studies executed by employing high resolution instruments such as scanning electron microscope equipped with field emission gun has been extremely useful to detect the rupture mechanism and deduce the typology and distributions of the significant defects involved into failure.

In order to evaluate the macroscopic fracture modality, additional low magnification observations have been performed; the regions of microscopic crack initiation and stable crack growth have been identified as well as the regions which presumably have been subjected to the final failure process or overloading effects.

The fine-scale topography and the microscopic mechanisms governing fracture needed to be characterized; for this purpose higher magnification observations

have been performed in the zones of early microscopic crack growth to identify the size, location and number of the microscopic cracks and their progression in the material microstructure. On the other hand, also the region of overload and final failure has been analysed in order to identify the fine-scale features reminiscent of the local governing mechanisms.

The fracture surfaces of the specimens tested between 0.4×10^6 and 3×10^6 cycles are shown in Fig. 10; it can be seen that in the high cycle loading range the fracture front is formed along the flow material lines produced by the tool during welding.

On the other hand, in both the low and high cycle load specimen regions the microscopic crack growth has been associated with some degree of material ductile behaviour, showing the typical fracture surfaces of very fine grain size structure into the welded section (Fig. 11).

Finally, in these micro-pictures small voids produced by the FSW process have been easily detected in the case of all the tensile tested specimens.

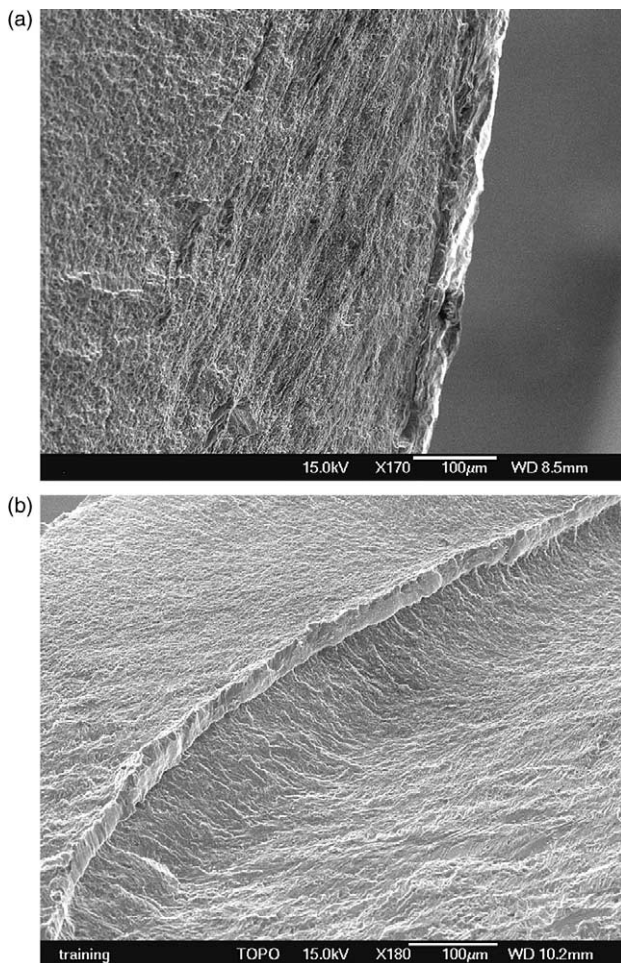


Fig. 10. Fracture surfaces of the fatigue specimens broken after 0.4×10^6 (a) and 3×10^6 cycles (b).

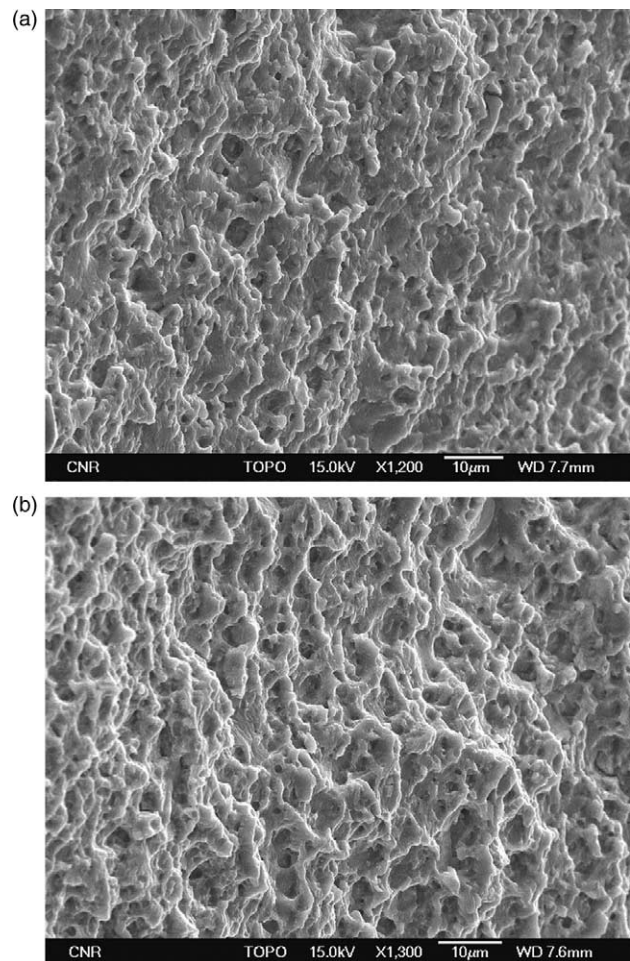


Fig. 11. Fracture surfaces of the fatigue specimens broken after 0.4×10^6 (a) and 3×10^6 cycles (b) showing the very fine grain structure of the material and microvoids produced by the process.

4. Conclusions

The dissimilar 2024 and 7075 aluminium alloys in the form of 2.5 mm thick sheets have been successfully joined by friction stir welding. The resulting microstructure has been widely investigated by optical microscopy, putting in evidence the grain structure and precipitates distribution differences originated by the process. Finally, the welded joints static and dynamic properties have been mechanically evaluated by means of tensile and fatigue tests. The presence of the FSW line reduces the fatigue behaviour but the comparison to the parent materials is acceptable and allows considering the FSW as an alternative joining technology for the aluminium sheet alloys. The specimens fracture surfaces after testing have been deeply analysed by using a FEGSEM microscope, revealing the defects typology and location after the Friction Stirring process and the microscopic mechanisms occurred during high stress deformations and final failure.

Acknowledgements

The authors would like to thank eng. Anna Eva Morabito of the University of Lecce for the fatigue data of the 2024T3 base material [19].

References

- [1] W.M. Thomas, E.D. Nicholas, J.C. Needam, M.G. Murch, P. Templesmith, C.J. Dawes, GB Patent Application No. 9125978.8, December 1991 and US Patent No. 5460317, October 1995.
- [2] G. Bussu, P.E. Irving, The role of residual stress and heat affected zone properties on fatigue crack propagation in friction stir welded 2024-T351 aluminium joints, *International Journal of Fatigue* 25 (2003) 77–88.
- [3] R. John, K.V. Jata, K. Sadananda, Residual stress effects on near threshold fatigue crack growth in friction stir welded aerospace alloys, *International Journal of Fatigue* 25 (2003) 939–948.
- [4] K.V. Jata, K.K. Sankaran, J. Ruschau, Friction stir welding effects on microstructure and fatigue of aluminium alloy 7050-T7451, *Metallurgical and Materials Transactions* 31A (2000) 2181–2192.
- [5] I. Charit, R.S. Mishra, M.W. Mahoney, Multi-sheet structures in 7475 aluminium by friction stir welding in concert with post-weld superplastic forming, *Scripta Materialia* 47 (2002) 631–636.
- [6] C.G. Rhodes, M.W. Mahoney, W.H. Bingel, M. Calabrese, Fine-grain evolution in friction-stir processed 7050 aluminium, *Scripta Materialia* 48 (2003) 1451–1455.
- [7] K.V. Jata, S.L. Semiatin, Continuous dynamic recrystallization during friction stir welding of high strength aluminium alloys, *Scripta Materialia* 43 (8) (2000) 743–749.
- [8] M. Guerra, C. Schmidt, J.C. McClure, L.E. Murr, A.C. Nunes, Flow patterns during friction stir welding, *Materials Characterization* 49 (2003) 95–101.
- [9] P. Ulysse, Three-dimensional modelling of the friction stir welding process, *International Journal of Machine Tools and Manufacture* 42 (2002) 1549–1557.
- [10] J.Q. Su, T.W. Nelson, R. Mishra, M. Mahoney, Microstructural investigation of friction stir welded 7050-T651 aluminium, *Acta Materialia* 51 (2003) 713–729.
- [11] C.G. Rhodes, M.W. Mahoney, W.H. Bingel, Effects of friction stir welding on microstructure of 7075 aluminium, *Scripta Materialia* 36 (1997) 69–75.
- [12] P. Cavaliere, E. Cerri, L. Marzoli, J. Dos Santos, Friction stir welding of ceramic particle reinforced aluminium based metal matrix composites, *Applied Composite Materials* 11 (4) (2004) 247–258.
- [13] Y.S. Sato, M. Urata, H. Kokawa, K. Ikeda, Hall-petch relationship in friction stir welds of equal channel angular-pressed aluminium alloys, *Materials Science and Engineering A354* (2003) 298–305.
- [14] P.B. Berbon, W.H. Bingel, R.S. Mishra, C.C. Bampton, M.W. Mahoney, Friction stir processing: a tool to homogenize nanocomposites aluminium alloys, *Scripta Materialia* 44 (2001) 61–66.
- [15] W.B. Lee, Y.M. Yeon, S.B. Jung, The improvement of mechanical properties of friction-stir-welded A356 Al alloy, *Materials Science and Engineering A355* (2003) 154–159.
- [16] I. Shigematsu, Y.J. Kwon, K. Suzuki, T. Imai, N. Saito, Joining of 5083 and 6061 aluminum alloys by friction stir welding, *Journal of Materials Science Letters* 22 (2003) 353–356.
- [17] W.-B. Lee, Y.-M. Yeon, S.-B. Jung, The joint properties of dissimilar formed Al alloys by friction stir welding according to the fixed location of materials, *Scripta Materialia* 49 (2003) 423–428.
- [18] J.A. Wert, Microstructures of friction stir weld joints between an aluminium-base metal matrix composite and a monolithic aluminium alloy, *Scripta Materialia* 49 (2003) 607–612.
- [19] A.E. Morabito, *Analisi termomeccanica degli effetti termoelastici e dissipativi associati al comportamento a fatica della lega di alluminio 2024T3*, PhD Thesis, Università di Lecce, 2003.